Intramitochondrial calcium regulation by the FHIT gene product sensitizes to apoptosis

Alessandro Rimessi[a], Saverio Marchi[a], Carmen Fotino[a], Anna Romagnoli[a], Kay Huebner[b], Carlo M. Croce[b,1], Paolo Pinton[a], and Rosario Rizzuto[a,c,1]

[a]Department of Experimental and Diagnostic Medicine, Interdisciplinary Center for the Study of Inflammation, and Emilia Romagna Laboratory BioPharmaNet Laboratory, University of Ferrara, 44100 Ferrara, Italy; [b]Department of Molecular Virology, Immunology, and Medical Genetics, Comprehensive Cancer Center, Ohio State University, Columbus, OH 43210; and [c]Department of Biomedical Sciences, University of Padua, 35121 Padua, Italy

Contributed by Carlo M. Croce, June 15, 2009 (sent for review March 10, 2009)

Despite the growing interest in the Fhit tumor suppressor protein, frequently deleted in human cancers, the mechanism of its powerful proapoptotic activity has remained elusive. We here demonstrate that Fhit sensitizes the low-affinity Ca^{2+} transporters of mitochondria, enhancing Ca^{2+} uptake into the organelle both in intact and in permabilized cells, and potentiating the effect of apoptotic agents. This effect can be attributed to the fraction of Fhit sorted to mitochondria, as a fully mitochondrial Fhit (a chimeric protein including a mitochondrial targeting sequence) retains the Ca^{2+} signaling properties of Fhit and the proapoptotic activity of the native protein (whereas the effects on the cell cycle are lost). Thus, the partial sorting of Fhit to mitochondria allows to finely tune the sensitivity of the organelle to the highly pleiomorphic Ca^{2+} signals, synergizing with apoptotic challenges. This concept, and the identification of the molecular machinery, may provide ways to act on apoptotic cell death and its derangement in cancer.

calcium signaling | mitochondria | oncosopressor | oxidative stress

The fragile histidine triad (*FHIT*) gene, isolated by positional cloning, encompasses the most common human fragile site FRA3B at 3p14.2. This chromosomal region is involved in hemizygous and homozygous deletions, and indeed mutations of *FHIT* were demonstrated in a large variety of human tumors (1–4). *FHIT* encodes a 17-kDa protein (Fhit) that is abundantly expressed in normal human lung, stomach, kidney, and other epithelial tissues, whereas most tumors and tumor-derived cell lines do not express Fhit or show markedly reduced levels of the protein (5). Fhit knock-out mice are more susceptible to cancer development than their wild-type counterparts (6), and *FHIT* gene therapy can prevent and reverse tumors in carcinogen-exposed Fhit-deficient mice (7). However, the precise molecular mechanism involved in the antitumor function of *FHIT* remains largely unclear.

Fhit is partly localized in mitochondria, and interaction with Hsp60/Hsp10 could be important for correct refolding after import and Fhit stability (8). This compartmentalization of Fhit could reveal a transcription-independent regulation of cell fate. Indeed, mitochondria are at the crossroad of numerous apoptotic pathways that synergize in triggering the morphological transitions underlying the release of proapoptotic factors into the cytoplasm (9–11). In most cases, Ca^{2+} acts as a fundamental sensitizing factor, and anti-apoptotic proteins, such as Bcl-2, have been shown to reduce ER Ca^{2+} levels, and agonist-dependent release and mitochondrial loading (12–14).

Different agents induce Ca^{2+} release from the ER Ca^{2+} store through the IP_3R Ca^{2+} release channel (15). Consequent mitochondrial Ca^{2+} uptake, via a yet unidentified Ca^{2+} channel of the inner mitochondrial membrane (the mitochondrial Ca^{2+} uniporter, MCU), regulates different processes: Aerobic metabolism (16), release of caspase cofactors (17), and feedback control of neighboring ER or plasma membrane Ca^{2+} channels (18, 19). The ER and mitochondria are thus crucial nodes at which intracellular Ca^{2+} fluxes and functional outcomes are governed (20). Their relevance to the control of cell survival is supported by several reports showing that modulation of mitochondrial Ca^{2+} accumulation (because of modification of the molecular repertoire of the cells) modifies cellular sensitivity to Ca^{2+}-mediated apoptotic stimuli (12–14).

We thus investigated whether Fhit has a role in the control of Ca^{2+} fluxes across the mitochondrial membranes. The results demonstrated that Fhit increases the affinity of the mitochondrial machinery for Ca^{2+} accumulation into the organelle, thus enhancing mitochondrial Ca^{2+} uptake triggered by physiological agonists and apoptotic challenges. The increase in mitochondrial Ca^{2+} loading, by favoring the elimination of altered or damaged cells by apoptosis, may play a key role in the mechanism of action of this important tumor suppressor.

Results

Subcellular Localization of Fhit and Effect on Ca^{2+}-Homeostasis. The intracellular location (Fig. 1*A*) and expression level (Fig. 1*B*) of endogenous and overexpressed Fhit were first verified. Immunofluorescence experiments revealed a diffuse cytosolic and nuclear staining and a stronger labeling of filamentous structures corresponding to mitochondria (as confirmed by the merged image with cotransfected mitochondrial GFP, mtGFP) (Fig. 1*A*). Upon overexpression, the fraction of nuclear Fhit appears increased, compared with the cytosol (compare Fig. 1*AI* and *AII*). Moreover, the mitochondrial staining of Fhit was confirmed also after permeabilization of the plasma membrane using digitonin to remove the cytosolic pool of the protein (Fig. 1*C*).

Then, calcium measurements were carried out, using aequorin-based recombinant probes (21). Fig. 1*D* shows the results of a typical experiment. Where indicated, HeLa cells were exposed to histamine (100 μM), causing the generation of inositol 1,4,5 trisphosphate (IP_3) and the consequent release of Ca^{2+} from the ER. No difference in cellular Ca^{2+} handling was observed between Fhit-overexpressing and control cells. Indeed, both groups of cells showed very similar luminal ER Ca^{2+} concentrations at rest ($[Ca^{2+}]_{er}$) (control: 461.00 $\pm$ 22.90 μM vs. Fhit: 471.50 $\pm$ 25.10 μM) and comparable release kinetics upon histamine addition. Accordingly, the transient rises of Ca^{2+} concentration in the cytosol ($[Ca^{2+}]_c$) and in the mitochondrial matrix ($[Ca^{2+}]_m$) elicited by the agonist were very similar ($[Ca^{2+}]_c$, control 2.82 $\pm$ 0.05 μM vs. Fhit 2.92 $\pm$ 0.08 μM; $[Ca^{2+}]_m$, control 82.20 $\pm$ 4.70 μM vs. Fhit 85.70 $\pm$ 3.79 μM). The situation changed at a lower agonist dose (10 μM histamine). The aequorin probes showed very similar release kinetics from the ER, slower than with 100 μM histamine (control 3.21 $\pm$ 0.40 μM/s vs. Fhit 3.32 $\pm$ 0.29 μM/s), and superimposable $[Ca^{2+}]_c$ peaks (control 2.67 $\pm$ 0.08 μM; Fhit 2.66 $\pm$ 0.08 μM) (Fig. 1*E*). Conversely, in Fhit-overexpressing cells, the $[Ca^{2+}]_m$ increase was approximately 30% greater (control 13.01 $\pm$ 0.75 μM vs. Fhit 16.74 $\pm$ 1.44 μM) (Fig. 1*E*). This effect was not cell type-specific, as the same results were obtained in A549 cells (Fig. S1*A*), nor could it be related to overexpressed

Author contributions: A. Rimessi, P.P., and R.R. designed research; A. Rimessi, S.M., C.F., and A. Romagnoli performed research; K.H. and C.M.C. contributed new reagents/analytic tools; A. Rimessi, S.M., C.F., A. Romagnoli, K.H., C.M.C., P.P., and R.R. analyzed data; and A. Rimessi, C.M.C., P.P., and R.R. wrote the paper.

The authors declare no conflict of interest.

[1]To whom correspondence may be addressed. E-mail: rosario.rizzuto@unipd.it or carlo.croce@osumc.edu.

This article contains supporting information online at www.pnas.org/cgi/content/full/0906484106/DCSupplemental.

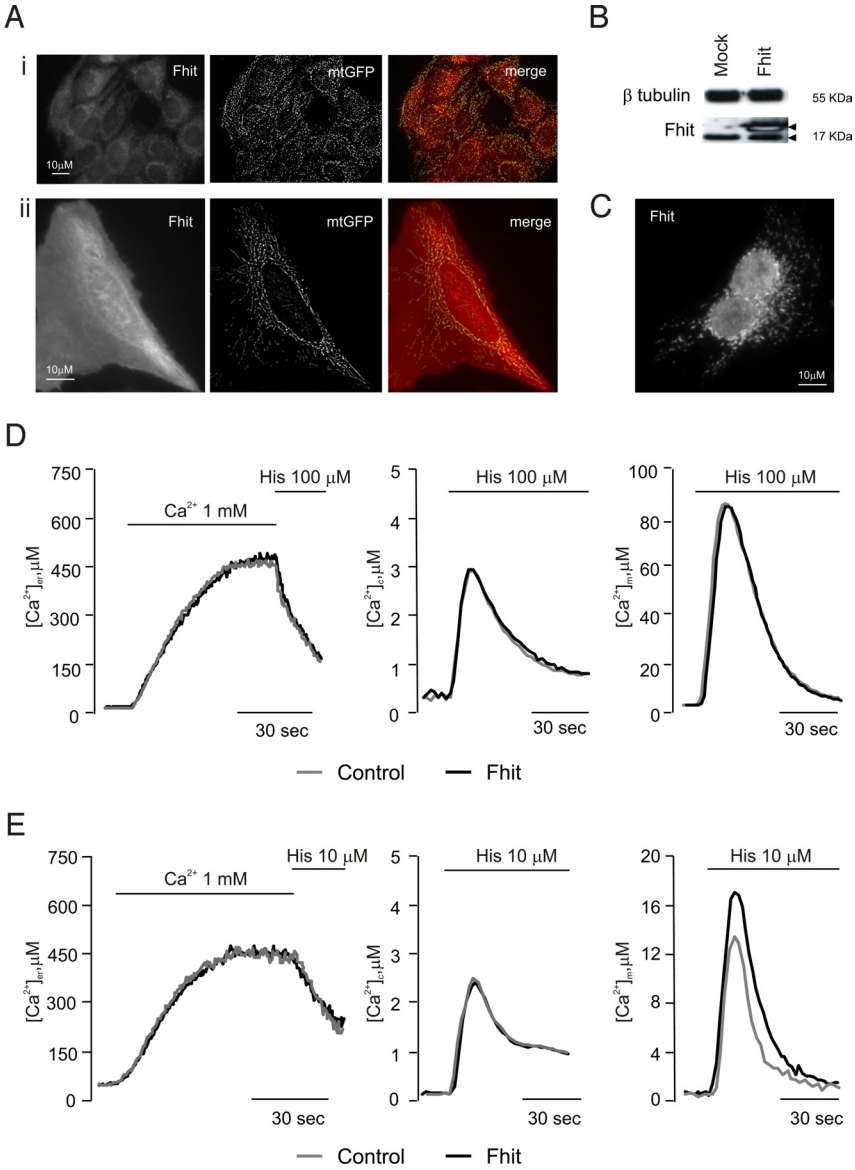

Fig. 1. Subcellular localization of Fhit and effect on Ca^{2+}−homeostasis. (*A*) Immunofluorescence labeling of Fhit (*Left*), mtGFP visualization (*Middle*), and merged image (*Right*) in HeLa cells. (*I*) Control, (*II*) Fhit-overexpressing cells. (*B*) Western blotting of Fhit and β tubulin as reference. Arrowheads denote the position of endogenous (lower) and His-6-tagged (higher) Fhit bands in mock-transfected (Mock) and Fhit-overexpressing (Fhit) HeLa cells. The level of overexpression is typical of the results obtained in all of the experiments of this paper. (*C*) Immunofluorescence labeling of overexpressed Fhit after plasma membrane permeabilization with digitonin. (*D* and *E*) $[Ca^{2+}]$ measurement in the ER (*Left*), cytosol (*Middle*), and mitochondria (*Right*) in controls (gray line) and Fhit-overexpressing cells upon 100 μM (*D*) and 10 μM (*E*) histamine. These and the following figures are representative of >10 experiments, giving similar results.

protein, as shRNA silencing of endogenous Fhit in HeLa cells caused the expected opposite effect (control 13.23 ± 1.92 μM vs. shRNA Fhit 10.93 ± 1.79 μM) (Fig. S1*B*).

Assessment of Mitochondrial Ca^{2+}-Uptake Capacity in Permeabilized and Intact Cells. We then investigated the possible mechanism of the increased uptake at submaximal agonist stimulation. Rapid uptake into mitochondria depends on close interactions with the ER (22, 23), as well as on the state of fusion/fission of the organelle network (24). 3D reconstruction of mtGFP-labeled of mitochondria showed no difference in distribution and shape between Fhit-overexpressing and control cells (Fig. S2*A*). As to the driving force for Ca^{2+} accumulation, loading of the potential-sensitive tetramethyl rhodamine methyl ester (TMRM) dye revealed no difference in the transmembrane potential (ΔΨ) (Fig. S2*B*). We thus concluded that the explanation of our results most likely resided in the increased affinity of the molecularly undefined transporter (the mitochondrial Ca^{2+} uniporter, MCU). We explored this possibility by measuring mitochondrial Ca^{2+} uptake in permeabilized cells and by visualizing the hotspots of rapid mitochondrial uptake in intact cells. In the former case, transfected HeLa cells were perfused with a solution mimicking the intracellular milieu (IB), supplemented with 2 mM EGTA, and permeabilized with 20 μM digitonin for 1 min. Then, the perfusion buffer was changed to IB with an EGTA-buffered $[Ca^{2+}]$ of 1 μM, eliciting a gradual rise in $[Ca^{2+}]_m$ that reached a plateau value of approximately 30 μM (Fig. 2*A*). In Fhit-overexpressing HeLa cells, the $[Ca^{2+}]$ increase was larger and faster than in controls (V_m, mean of first 15 s, control: 0.53 ± 0.01 μM/s vs. Fhit: 0.79 ± 0.01 μM/s) and reached an approximately 20% higher plateau.

A coherent picture emerged from single-cell imaging experiments in HeLa cells with a GFP-based mitochondrial probe, 2 mtRP (25). Time-lapse series of high resolution images were acquired at 5–10 frame/s and visualized as 2D image series of the whole mitochondrial network. These data allowed calculation of the number of localized $[Ca^{2+}]_m$ increases (hotspots), visualized in a pseudocolor scale, and evaluation of their diffusion across mitochondria. After application of 10 μM histamine, mitochondrial Ca^{2+} uptake initiated at preferential points of the mitochondrial network and the $[Ca^{2+}]$ increase traveled along the mitochondrial profiles, saturating the relatively high-affinity probe. In Fhit-overexpressing cells, the number of hotspots was markedly greater than in controls (Fig. 2*B*). This heterogeneity, and the increased number of hotspots in Fhit-overexpressing cells, was quantified by calculating the standard deviation of the relative fluorescence changes over individual mitochondrial objects (control 10.55 ± 0.95 versus Fhit 16.06 ± 1.45, $P < 0.01$; Fig. 2*C*).

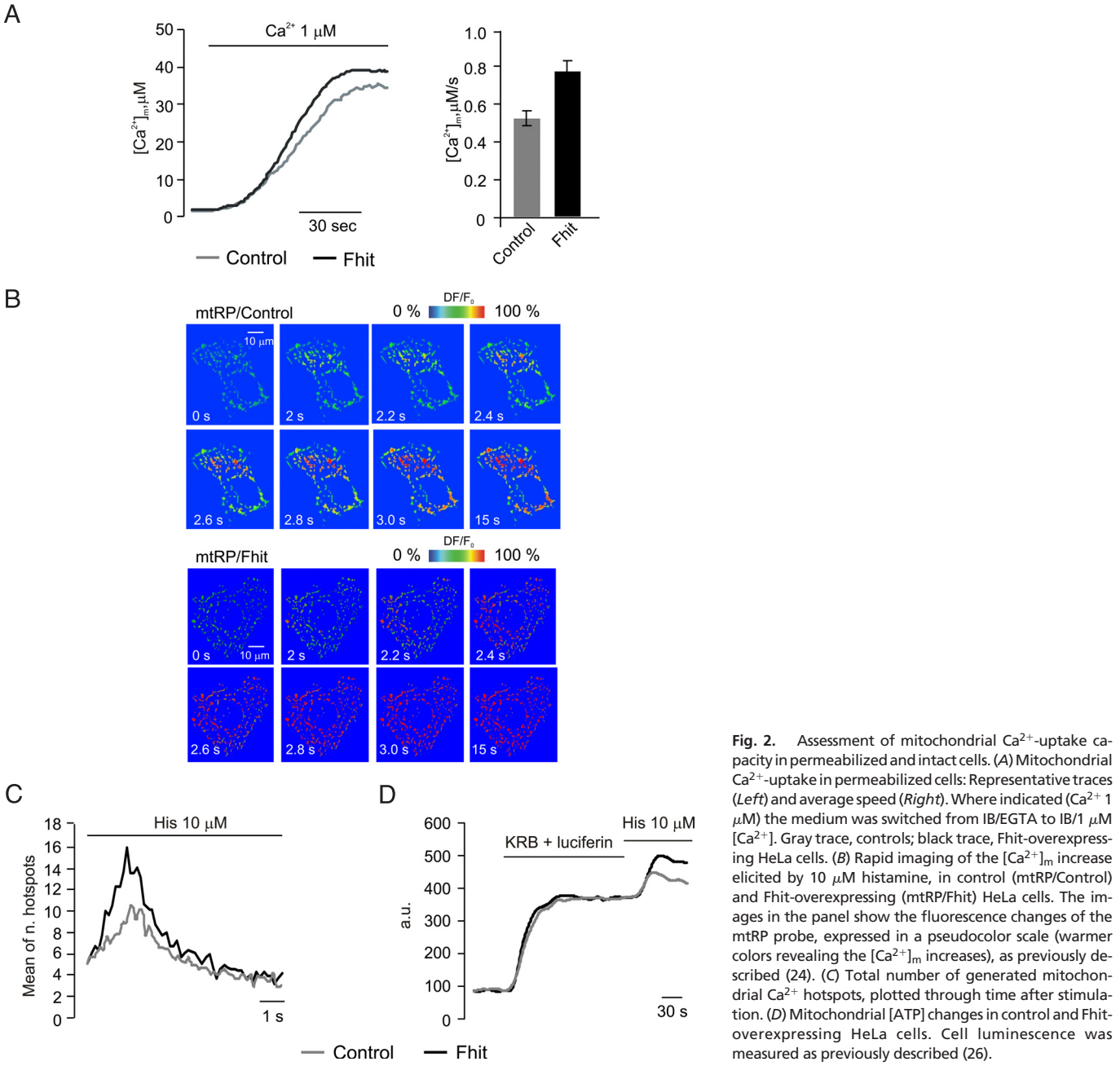

Fig. 2. Assessment of mitochondrial Ca^{2+}-uptake capacity in permeabilized and intact cells. (*A*) Mitochondrial Ca^{2+}-uptake in permeabilized cells: Representative traces (*Left*) and average speed (*Right*). Where indicated (Ca^{2+} 1 μM) the medium was switched from IB/EGTA to IB/1 μM [Ca^{2+}]. Gray trace, controls; black trace, Fhit-overexpressing HeLa cells. (*B*) Rapid imaging of the $[Ca^{2+}]_m$ increase elicited by 10 μM histamine, in control (mtRP/Control) and Fhit-overexpressing (mtRP/Fhit) HeLa cells. The images in the panel show the fluorescence changes of the mtRP probe, expressed in a pseudocolor scale (warmer colors revealing the $[Ca^{2+}]_m$ increases), as previously described (24). (*C*) Total number of generated mitochondrial Ca^{2+} hotspots, plotted through time after stimulation. (*D*) Mitochondrial [ATP] changes in control and Fhit-overexpressing HeLa cells. Cell luminescence was measured as previously described (26).

Based on previous observations that stimulations with agonists evoking mitochondrial Ca^{2+} signals cause parallel increases in intracellular ATP (26), we also measured mitochondrial ATP levels ($[ATP]_m$) in control and Fhit-overexpressing HeLa cells. For this purpose, the mitochondria-targeted ATP probe luciferase (mtLUC) was cotransfected, as previously reported (26) (Fig. 2*D*). Interestingly, overexpression of Fhit increases the $[ATP]_m$ rise evoked by 10 μM histamine, thus demonstrating that (i) also at submaximal agonist challenges the $[Ca^{2+}]_m$ rise is decoded into a stimulation of mitochondrial aerobic metabolism and (ii) Fhit plays a role in the metabolic effect of mitochondrial Ca^{2+} signals.

The $[Ca^{2+}]_m$ Is Affected by a Mitochondrial Fhit Chimera. We then investigated whether the mitochondrial signaling alteration is caused by the fraction of Fhit protein localized to mitochondria. To fully sort Fhit to mitochondria, a mitochondrial targeting sequence was appended at its N terminus (mtFhit; Fig. 3*A*). Indeed, immunofluorescence experiments showed only the typical filamentous structure of the mitochondrial network (Fig. 3*A*). We then carried out mitochondrial Ca^{2+} measurements, using the mtAEQ, erAEQ, and cytAEQ probes, cotransfected with mtFhit (mtFhit). Upon submaximal histamine challenge (10 μM), mtFhit-overexpressing cells underwent a $[Ca^{2+}]_m$ rise that was markedly greater than that of controls and comparable to that of Fhit-overexpressing cells (mtFhit 16.53 $\pm$ 1.85 μM), whereas the $[Ca^{2+}]_{er}$ and $[Ca^{2+}]_c$ values were comparable to those of control cells. These data show that a Fhit variant with exclusive mitochondrial localization fully retains the effect on mitochondrial Ca^{2+} signaling of the wild-type protein (Fig. 3*B*). We then labeled the ER and the mitochondria with a GFP-based probe (erGFP) and MitoTracker-Red to investigate organelle morphology in mtFhit-transfected and control cells. No alteration was observed in the morphology of the 2 organelles nor in the number and location of the contacts (Fig. S3*A*). Then $\Delta\Psi$ was measured with TMRM, used as described in Fig. S2*B*. Also in this case, no difference was observed between mtFhit-expressing and control

CELL BIOLOGY

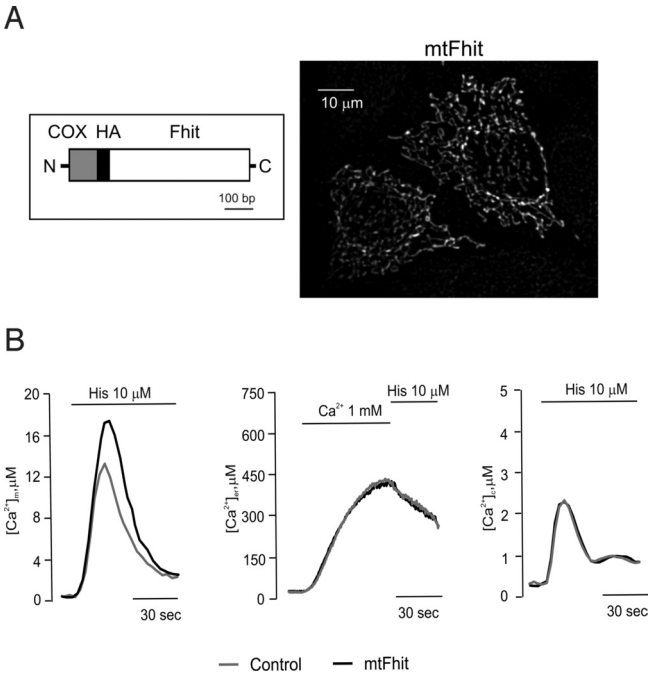

Fig. 3. Subcellular localization and effect on Ca^{2+} signaling of mtFhit. (*A*) Map of the mtFhit cDNA and immunolocalization of the expressed protein. (*B*) $[Ca^{2+}]$ measurement in the mitochondria, ER (control 438 ± 26.90 μM vs. Fhit 411 ± 35.60 μM), and cytosol (control 2.48 ± 0.03 μM vs. Fhit 2.50 ± 0.03 μM) in controls (gray) and mtFhit-overexpressing cells (black) upon addition of 10 μM histamine.

cells (Fig. S3*B*). We thus concluded that mtFhit does not exert damaging effects on mitochondrial morphology, on the functional interaction with the ER, and in the generation of the membrane potential across the inner membrane.

The Mitochondrial Fraction of Fhit Potentiates Apoptotic Effect of Menadione. We then investigated the functional consequences of the signaling alteration. Various apoptotic challenges appear to use Ca^{2+} as a sensitizing cofactor, e.g., C_2-ceramide, oxidative stress (menadione, H_2O_2) or arachidonic acid (19, 27–29). These stimuli induce movement of Ca^{2+} from the ER to mitochondria, leading to Ca^{2+} overload, OMM permeabilization, and caspase-mediated cell death. To verify whether Fhit affects Ca^{2+} homeostasis and cell survival in apoptotic conditions, we investigated the effects of menadione. Treatment with menadione caused a small, transient $[Ca^{2+}]_c$ rise followed by a lower, sustained plateau (Fig. 4*A*). As expected, this low-amplitude $[Ca^{2+}]_c$ increase correlated with a marginal uptake of Ca^{2+} into mitochondria (Fig. 4*B*). Interestingly, also in the case of the apoptotic challenge the $[Ca^{2+}]_m$, but not the $[Ca^{2+}]_c$ rise, was markedly greater in Fhit-overexpressing cells. We then correlated the Ca^{2+} data with the efficacy of the oxidizing agent in causing cell death, by 2 approaches: the microscopic assessment of cell survival (apoptotic counts), after coexpression of a fluorescent marker (mtGFP), and Annexin V-based measurement of apoptosis. In the first case, a decrease in the percentage of fluorescent cells correlates with a proapoptotic role of the expressed protein (30). As expected, after menadione treatment a substantial reduction in the number of Fhit-overexpressing cells was observed (control Δ% 1.94 ± 6.75 vs. Fhit −36.79 ± 7.25) (Fig. 4*C*). Similar results were obtained with other Ca^{2+}-mediated apoptotic challenges, such as H_2O_2 (Fig. S4*A*). Interestingly, the reduction was even greater with mtFhit (Δ% −45.48 ± 7.39). In Annexin V measurements, Fhit-overexpressing and control cells were labeled with Alexa Fluor 488 Annexin V, sorted by flow cytometry, and expressed as percentage of strongly fluorescent cells (Fig. 4*D*). In basal conditions, higher levels of Annexin V labeling were detected in Fhit-overexpressing HeLa cells (21.1%) compared with controls (13%). After a 2-h treatment with menadione, the percentage of Annexin-positive cells increased to 38.3% (16.6% of nontransfected cells). With mtFhit, the percentage of Annexin V-positive cells was comparable to controls in basal conditions (12%), but was greatly measured after treatment with menadione (16.6%, 38.3%, and 52.5% for control, Fhit, and mtFhit-transfected cells, respectively). Overall, these data indicate that mitochondrially localized Fhit does not influence basal levels of apoptosis, but greatly sensitizes to apoptotic challenges, in good agreement with the view of a Ca^{2+}-mediated intramitochondrial potentiation of apoptotic routes. Accordingly, no potentiation by Fhit was detected when the cells were challenged with a Ca^{2+}-independent apoptotic stimulus, such as staurosporine (Fig. S4*B*).

Finally, we investigated whether other putative functions of Fhit, which have been proposed to cooperate in tumor suppression but are unlikely to be ascribed to a mitochondrial effect, are also shared by mtFhit. We focused on cell cycle control (31) and carried out FACS sorting of cells after DNA labeling with propidium iodide (Fig. 4*E*). Fhit-overexpressing cells showed an increased number of cells in the G_2 phase or at the S-G_2 boundary, as reported in H460 cells (32). Conversely, mtFhit does not share this property with Fhit, as the distribution of cells in G0/G1, S, and G2/M is very similar to that of control cells (G0/G1: 48.4%, 35.1%, 47.1%; S: 8.2%, 9.6%, 7.9%; G2/M: 36.8%, 42.7%, 36.4% for control, Fhit, and mtFhit-transfected cells, respectively).

Discussion

Our previous observation that Fhit protein is localized within mitochondria and engages protein-protein interactions with resident proteins such as ferredoxin (8) highlighted the possibility that it could tune apoptotic signals reaching the mitochondrial checkpoint. We pursued this hypothesis, focusing on Ca^{2+} signaling, based on a large body of experimental evidence by us and other groups that demonstrates the importance of mitochondrial Ca^{2+} loading for triggering the morphological transitions of apoptosis (10, 11, 33, 34). The results were very striking, as not only they revealed a marked potentiation of the matrix $[Ca^{2+}]$ transients elicited by physiological stimuli and apoptotic agents, but also identified a mechanism for this effect.

Fhit is an enigmatic protein, exerting an AP3Ahydrolase activity that is not required for its tumor suppression function (35). To date, the exact mechanism by which Fhit exerts its antitumor activity remains obscure. A considerable body of evidence points to the role of Fhit in apoptosis induction and cell cycle regulation, including its role as modulator of DNA damage checkpoint response (36), but the molecular pathways of the apoptotic activity of Fhit remain elusive. Our results bring this tumor suppressor to the core mechanism of the intrinsic pathway of apoptosis, participating in the regulation of the critical mitochondrial steps. This effect is mediated by the fraction of Fhit localized in mitochondria (8), whereas other reported functions of Fhit, such as the putatively transcriptional control of the cell cycle are unaffected by an exclusively mitochondrial Fhit chimera. These data thus suggest that the complex intracellular distribution of Fhit may underlie a synergistic effect of different protein pools (cell cycle block, induction of apoptosis) that cooperate in repairing or eventually clearing DNA-damaged cells.

As to the mechanism itself, the data provide a radically different picture from the numerous previous examples of pro and anti-apoptotic proteins acting on calcium signaling. The $[Ca^{2+}]_{ER}$ levels were shown to be modulated by the Bcl-2 family members, with Bcl-2 itself reducing the state of filling of the Ca^{2+} store (14), and Bax and Bak counteracting this effect (28). In turn, the partial emptying reduces mitochondrial Ca^{2+} loading and, hence, the efficacy of various apoptotic challenges (17, 28). In the case of neurodegenerative signals and of the proapoptotic HBx protein, mitochondrial Ca^{2+} overload was shown to depend on the caspase-mediated cleavage of the plasma membrane Ca^{2+} ATPase (PMCA) that impairs the termination mechanism of the Ca^{2+} signal and amplifies and extends the cytosolic Ca^{2+} increases (37, 38).

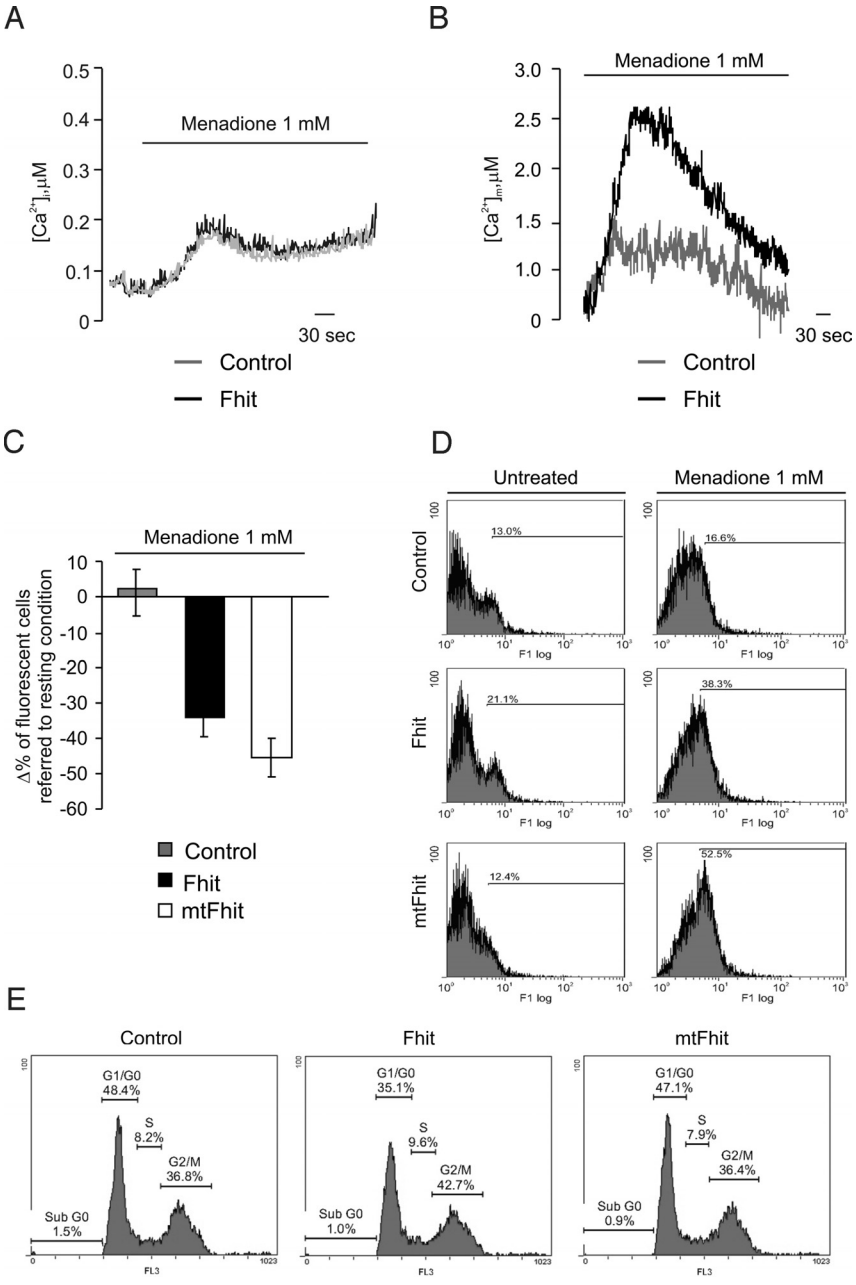

Fig. 4. The mitochondrial fraction of Fhit potentiates apoptotic challenges. (*A*) $[Ca^{2+}]_c$ and (*B*) $[Ca^{2+}]_m$ increases elicited by 1 mM menadione. (*C* and *D*) Assessment of cell viability via apoptotic counts (*C*) or Annexin V labeling (*D*) in controls, Fhit and mtFhit overexpressing cells, as indicated. In panel *D*, the percentage of cells over a common arbitrary level of fluorescence is indicated. (*E*) Distribution of HeLa cells in the cell cycle, as estimated by propidium iodide staining of DNA. The percentage of cells in G0/G1, S, and G2 is reported in each graph.

Here, we report that Fhit does not alter cytoplasmic Ca^{2+} signals and acts specifically on mitochondria by modifying the affinity of the MCU. Accordingly, mitochondrial Ca^{2+} signals are minimally affected by supramaximal agonist stimulations, but are markedly increased at lower, more physiological agonist concentrations.

This mechanism of action appears very effective in apoptosis for 2 reasons. The first reason is that apoptotic challenges, such as the lipid mediator C2-ceramide (17) and oxidative stress, such as that caused by menadione or H_2O_2 and used in this paper, have been shown to empty Ca^{2+} stores, but do so with a slow kinetics. Accordingly, mitochondrial uptake is relatively modest, because the low affinity of the MCU requires the generation of high $[Ca^{2+}]$ microdomains at the ER/mitochondria contacts (22, 23). If, however, the affinity of the MCU is increased by Fhit, also under those conditions mitochondria accumulate a large Ca^{2+} load, allowing the opening of the PTP and the induction of cell death, as directly shown in the experiment of Fig. 4.

In addition, physiological Ca^{2+}-mediated signals may synergize with PTP sensitizers (e.g., ceramide or alcohol), initiating slow waves of depolarization and Ca^{2+} release propagating through the cell (27). In this picture, Fhit, by sensitizing mitochondria, increases the possibility that any stimulatory input to the cell reaches the threshold for initiating the apoptotic Ca^{2+} wave. The observation of Fig. 2 that Fhit increases the number of hotspots (i.e., initial sites of Ca^{2+} uptake in mitochondria) strongly supports this scenario.

Finally, the identification of Fhit as a protein modulator of the MCU can open the way to proteomic approaches for solving the molecular enigma of mitochondrial Ca^{2+} homeostasis. Indeed, despite the growing interest in this process, the MCU remains undefined at the molecular level, and all of the efforts for biochemically identifying it have been frustrated by the lack of specific tools for labeling the proteins (the best characterized inhibitor, Ruthenium Red, binds unspecifically to a wide array of proteins). The demonstration that Fhit binds, directly or indirectly, to the MCU gives the possibility of analyzing the mitochondrial complexes in which it is engaged, with the aim of identifying the molecular component(s) of the MCU.

CELL BIOLOGY

Overall, understanding the mechanisms through which Ca^{2+} signals can be shifted from regulators of cellular functions to pathological effectors and the role of mitochondria as decisive checkpoints is an exciting task in biomedical research and a promising opportunity for developing drugs. The observation that Fhit is directly engaged in this process deepens our insight into the functioning of this important tumor suppressor and further stresses the relevance of mitochondrial Ca^{2+} homeostasis in cancer-related apoptosis.

Materials and Methods

Cell Culture, Ca^{2+} Measurements, and Immunodetection. For Fhit overexpression, an His-tagged recombinant protein construct (Fhit-His-6) was used; in all of the experiments carried out in HeLa cells, Fhit or mtFhit were overexpressed by transient transfection. For Fhit overexpression in A549 cells and Fhit shRNA silencing in HeLa cells, adenoviral (AdFhit: Fhit-His-6-pAdenoVator-CMV5-IRES-GFP, AdmtGFP: mtGFP-pAdEasy) and lentiviral (shRNA Fhit: shRNAFhit-pLKO.1) vectors were used, respectively, in association with adenoviral vectors for the expression of the aequorin probes (AdmtAEQ: mtAEQ-pAdEasy).

HeLa cell culture, transfection with aequorin-based (erAEQmut, cytAEQ, and mtAEQmut) or GFP-based (mtGFP, 2mtRP) probes and Fhit, and Ca^{2+} measurements were carried out exactly as previously described (22). Images of fluorescent indicators (mtGFP, TMRM, 2mtRP) were acquired from cells placed in thermostated chambers on the stage of a digital or confocal microscope and processed, as previously described (24). Specifically, for the images of Fig. 2*B*, the first deconvoluted image in the series was used as threshold to create a binary mask, allowing visualization of only the mitochondrial network. dF/F images were calculated from the original images and were multiplied by the binary mask with the image arithmetic functions of the MetaMorph software. Image scaling and pseudocolors were applied with the MetaFluor Analyst software of the Meta Imaging software package. In the experiments of Fig. 2*A*, Fhit-transfected and control HeLa cells were transferred to IB buffer (140 mM KCl, 10 mM NaCl, 1 mM K_3PO_4, 5.5 mM glucose, 2 mM $MgSO_4$, 1 mM ATP, 2 mM sodium succinate, and 20 mM HEPES, pH 7.05, at 37 °C), supplemented with 2 mM EGTA, then permeabilized by supplementing the perfusion medium with 20 μM digitonin for 1 min, and perfused again with IB/EGTA. After transfer to the luminometer chamber, Ca^{2+} uptake into mitochondria was initiated by replacing IB/EGTA with IB containing a 2 mM EGTA-buffered [Ca^{2+}] of 1 μM, prepared as elsewhere described (30).

Immunofluorescence and immunoblotting were performed with Fhit antiserum (Zymed Laboratories) (39) and anti β-tubulin (Santa Cruz Biotechnology), according to standard procedures (40).

Plasmid Construction. For constructing mtFhit, an in frame *Hin*dIII site and the HA1 tag were added via suitable PCR primers, then the HA-Fhit coding sequence was ligated to the mitochondrial targeting sequence (derived from subunit VIII of COX) excised from mtAEQ (41). The final construct was cloned into the pcDNA3.1 expression vector.

Functional Analyses. Apoptosis was quantified by 2 approaches. In the first approach, the mtGFP fluorescent marker was coexpressed with Fhit or mtFhit, and effect on cell survival was estimated by calculating the fraction of fluorescent cells in the surviving population after an apoptotic challenge (2 h of treatment with 1 mM menadione, 1 mM H_2O_2, or 1 μM staurosporine for 3 h), exactly as described in previous papers for other genes of interest (30). Ten different fields per coverslip (taken with an objective 20×) were analyzed, and a mean per condition was extracted. The results were obtained from at least 3 coverslips per condition and expressed as variation in the percentage of fluorescent cells. In the second, after the menadione challenge, control cells or cells overexpressing Fhit or mtFhit were incubated with the Alexa Fluor 488 Annexin V antibody kit, according to the instruction of the producer (Molecular Probes), then sorted with a FACStar flow cytometer (Becton Dickinson). For cell cycle analyses, control or transfected cells were washed twice with cold ethanol, then resuspended in 0.1 mg/mL propidium iodide/Triton X-100 staining solution (0.1% Triton X-100, 20 mg/mL DNase-free RNase A), and analyzed by flow cytometry, as described above.

ACKNOWLEDGMENTS. Funding was provided from the Italian Ministry of Education, University and Research, The European Union (FP7 ''MyoAGE''), the Italian Association for Cancer Research, Telethon, the Italian Space Agency, National Institutes of Health Grant 1P01AG025532–01A1, the Italian Multiple Sclerosis Foundation, the Regional Program for Industrial Research, Innovation and Technology Transfer program of the Emilia Romagna Region, the ''Cariparo'' Foundation, and the United Mitochondrial Disease Foundation.

1. Huebner K, Croce CM (2003) Cancer and the FRA3B/FHIT fragile locus: It's a HIT. *Br J Cancer* 88:1501–1506.
2. Huebner K, Croce CM (2001) FRA3B and other common fragile sites: The weakest links. *Nat Rev Cancer* 1:214–221.
3. Ohta M, et al. (1996) The FHIT gene, spanning the chromosome 3p14.2 fragile site and renal carcinoma-associated t(3;8) breakpoint, is abnormal in digestive tract cancers. *Cell* 84:587–597.
4. Toledo G, Sola JJ, Lozano MD, Soria E, Pardo J (2004) Loss of FHIT protein expression is related to high proliferation, low apoptosis and worse prognosis in non-small-cell lung cancer. *Mod Pathol* 17:440–448.
5. Pekarsky Y, Palamarchuk A, Huebner K, Croce CM (2002) FHIT as tumor suppressor: Mechanisms and therapeutic opportunities. *Cancer Biol Ther* 1:232–236.
6. Zanesi N, et al. (2001) The tumor spectrum in FHIT-deficient mice. *Proc Natl Acad Sci USA* 98:10250–10255.
7. Dumon KR, et al. (2001) FHIT gene therapy prevents tumor development in Fhit-deficient mice. *Proc Natl Acad Sci USA* 98:3346–3351.
8. Trapasso F, et al. (2008) Fhit interaction with ferredoxin reductase triggers generation of reactive oxygenspecies and apoptosis of cancer cells. *J Biol Chem* 283:13736–13744.
9. Bernardi P, et al. (2006) The mitochondrial permeability transition from in vitro artifact to disease target. *FEBS J* 273:2077–2099.
10. Pinton P, Giorgi C, Siviero R, Zecchini E, Rizzuto R (2008) Calcium and apoptosis: ER-mitochondria Ca^{2+} transfer in the control of apoptosis. *Oncogene* 27:6407–6418.
11. Hajnóczky G, Davies E, Madesh M (2003) Calcium signaling and apoptosis. *Biochem Biophys Res Commun* 304:445–454.
12. Rong YP, et al. (2008) Targeting Bcl-2-IP3 receptor interaction to reverse Bcl-2's inhibition of apoptotic calcium signals. *Mol Cell* 31:255–265.
13. White C, et al. (2005) The endoplasmic reticulum gateway to apoptosis by Bcl-X(L) modulation of the InsP3R. *Nat Cell Biol* 7:1021–1028.
14. Pinton P, et al. (2000) Reduced loading of intracellular Ca^{2+} stores and downregulation of capacitative Ca^{2+} influx in Bcl-2-overexpressing cells. *J Cell Biol* 148:857–862.
15. Berridge MJ, Bootman MD, Roderick HL (2003) Calcium signalling: Dynamics, homeostasis and remodelling. *Nat Rev* Mol Cell Biol 4:517–529.
16. Hajnóczky G, Robb-Gaspers LD, Seitz MB, Thomas AP (1995) Decoding of cytosolic calcium oscillations in the mitochondria. *Cell* 82:415–424.
17. Pinton P, et al. (2001) The Ca^{2+} concentration of the endoplasmic reticulum is a key determinant of ceramide-induced apoptosis: Significance for the molecular mechanism of Bcl-2 action. *EMBO J* 20:2690–2701.
18. Hajnóczky G, Hager R, Thomas AP (1999) Mitochondria suppress local feedback activation of inositol 1,4,5-trisphosphate receptors by Ca2+. *J Biol Chem* 274:14157–14162.
19. Gilabert JA, Parekh AB (2000) Respiring mitochondria determine the pattern of activation and inactivation of the store-operated Ca(2+) current I(CRAC). *EMBO J* 19:6401–6407.
20. Giorgi C, De Stefani D, Bononi A, Rizzuto R, Pinton P (2009) Structural and functional link between the mitochondrial network and the endoplasmic reticulum. *Int J Biochem Cell Biol* Apr 21. [Epub ahead of print].
21. Pinton P, Rimessi A, Romagnoli A, Prandini A, Rizzuto R (2007) Biosensors for the detection of calcium and pH. *Methods Cell Biol* 80:297–325.
22. Rizzuto R, et al. (1998) Close contacts with the endoplasmic reticulum as determinants of mitochondrial Ca^{2+} responses. *Science* 280:1763–1766.
23. de Brito OM, Scorrano L (2008) Mitofusin 2 tethers endoplasmic reticulum to mitochondria. *Nature* 456:605–610.
24. Szabadkai G, et al. (2004) Drp-1-dependent division of the mitochondrial network blocks intraorganellar Ca^{2+} waves and protects against Ca^{2+}-mediated apoptosis. *Mol Cell* 16:59–68.
25. Filippin L, Magalhães P, Di Benedetto G, Colella M, Pozzan T (2003) Stable interactions between mitochondria and endoplasmic reticulum allow rapid accumulation of calcium in a subpopulation of mitochondria. *J Biol Chem* 278:39224–39234.
26. Jouaville LS, Pinton P, Bastianutto C, Rutter GA, Rizzuto R (1999) Regulation of mitochondrial ATP synthesis by calcium: Evidence for a long-term metabolic priming. *Proc Natl Acad Sci USA* 96(24):13807–13812.
27. Pacher P, Hajnóczky G (2001) Propagation of the apoptotic signal by mitochondrial waves. *EMBO J* 20:4107–4121.
28. Scorrano L, et al. (2003) BAX and BAK regulation of endoplasmic reticulum Ca^{2+}: A control point for apoptosis. *Science* 300:135–139.
29. Szado T, et al. (2008) Phosphorylation of inositol 1,4,5-trisphosphate receptors by protein kinase B/Akt inhibits Ca^{2+} release and apoptosis. *Proc Natl Acad Sci USA* 105:2427–2432.
30. Rapizzi E, et al. (2002) Recombinant expression of the voltage-dependent anion channel enhances the transfer of Ca^{2+} microdomains to mitochondria. *J Cell Biol* 159:613–624.
31. Ishii H, et al. (2005) Components of DNA damage checkpoint pathway regulate UV exposure-dependent alterations of gene expression of FHIT and WWOX at chromosome fragile sites. *Mol Cancer Res* 3:130–138.
32. Roz L, Gramegna M, Ishii H, Croce CM, Sozzi G (2002) Restoration of fragile histidine triad (FHIT) expression induces apoptosis and suppresses tumorigenicity in lung and cervical cancer cell lines. *Proc Natl Acad Sci USA* 99:3615–3620.
33. Duchen MR (2000) Mitochondria and calcium: From cell signalling to cell death. *J Physiol.* 529:57–68.
34. Brenner C (2002) Hint, Fhit and GalT: Function, structure, evolution, and mechanism of three branches of the histidine triad superfamily of nucleotide hydrolases and transferases. *Biochemistry* 41:9003–9014.
35. Giorgi C, Romagnoli A, Pinton P, Rizzuto R (2008) Ca2+ signaling, mitochondria and cell death. *Curr Mol Med* 8:119–130.
36. Zanesi N, et al. (2001) The tumor spectrum in *FHIT*-deficient mice. *Proc Natl Acad Sci USA* 98:10250–10255.
37. Chami M, Ferrari D, Nicotera P, Paterlini-Bréchot P, Rizzuto R (2003) Caspase-dependent alterations of Ca2+ signaling in the induction of apoptosis by hepatitis B virus X protein. *J Biol Chem* 278:31745–31755.
38. Bano D, et al. (2005) Cleavage of the plasma membrane Na+/Ca2+ exchanger in excitotoxicity. *Cell* 120:275–285.
39. Sozzi G, et al. (1996) The FHIT gene 3p14.2 is abnormal in lung cancer. *Cell* 85:17–26.
40. Rimessi A, et al. (2005) Inhibitory interaction of the 14–3-3ε protein with isoform 4 of the plasma membrane Ca^{2+}-ATPase pump. *J Biol Chem* 280:37195–37203.
41. Rizzuto R, Simpson AW, Brini M, Pozzan T (1992) Rapid changes of mitochondrial Ca^{2+} revealed by specifically targeted recombinant aequorin. *Nature* 358:325–327.

Supporting Information

Rimessi et al. 10.1073/pnas.0906484106

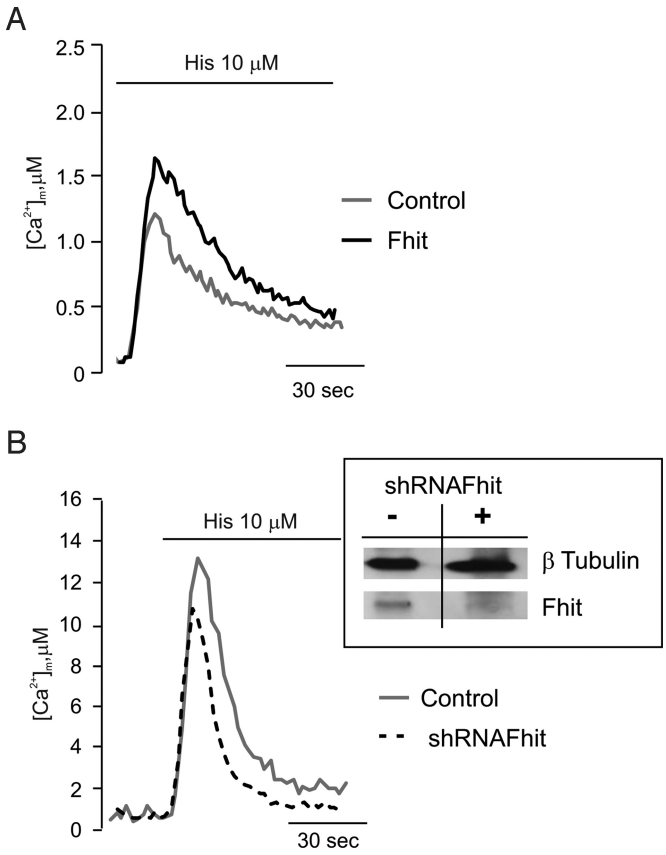

Fig. S1. (*A*) $[Ca^{2+}]_m$ measurements in control and in Fhit-transduced A549 cells after stimulation with histamine 10 μM. (*B*) $[Ca^{2+}]_m$ measurements in control and shRNA-Fhit-transduced HeLa cells. *Inset*, Fhit immunoblotting to estimate the level of shRNA-Fhit silencing.

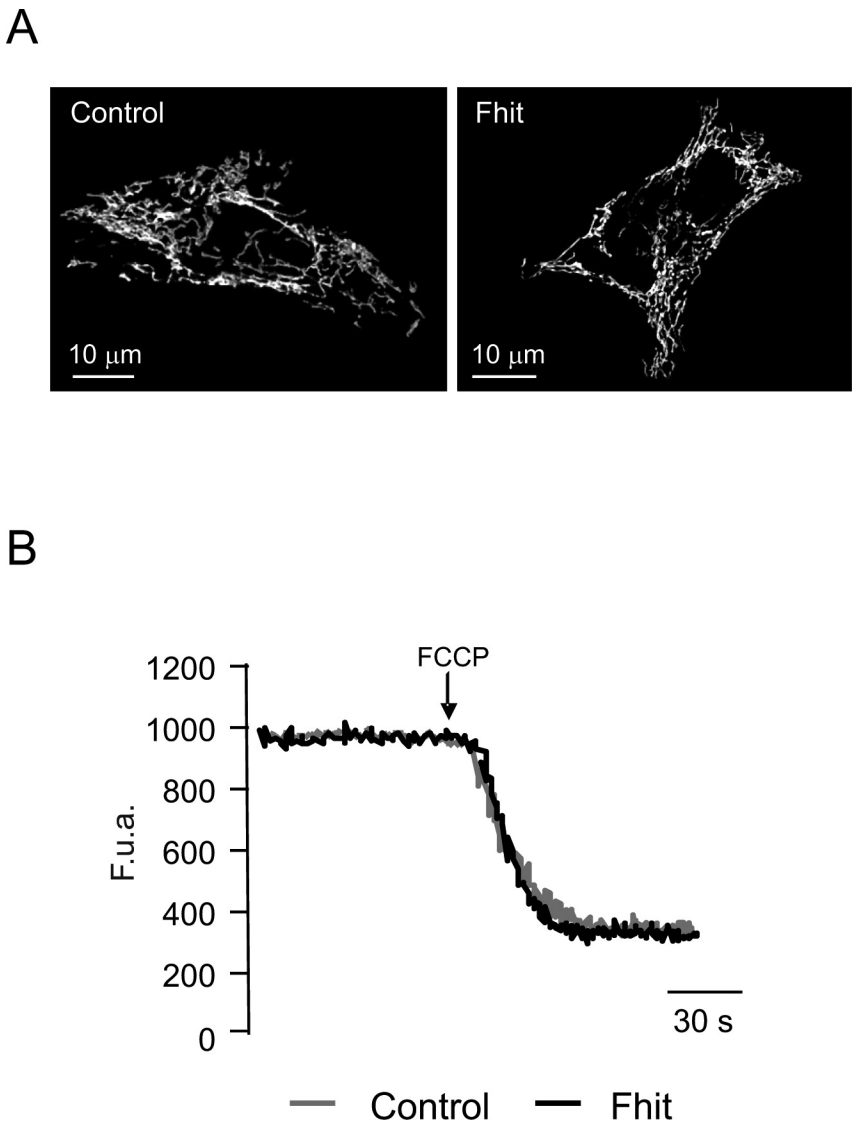

Fig. S2. (*A*) Mitochondrial morphology in Fhit-transfected and control HeLa cells as revealed by mtGFP visualization. (*B*) TMRM fluorescence level of control and Fhit cells, before and after treatment with FCCP (carbonyl cyanide *p*-trifluoromethoxyphenylhydrazone), to collapses $\Delta\Psi_m$.

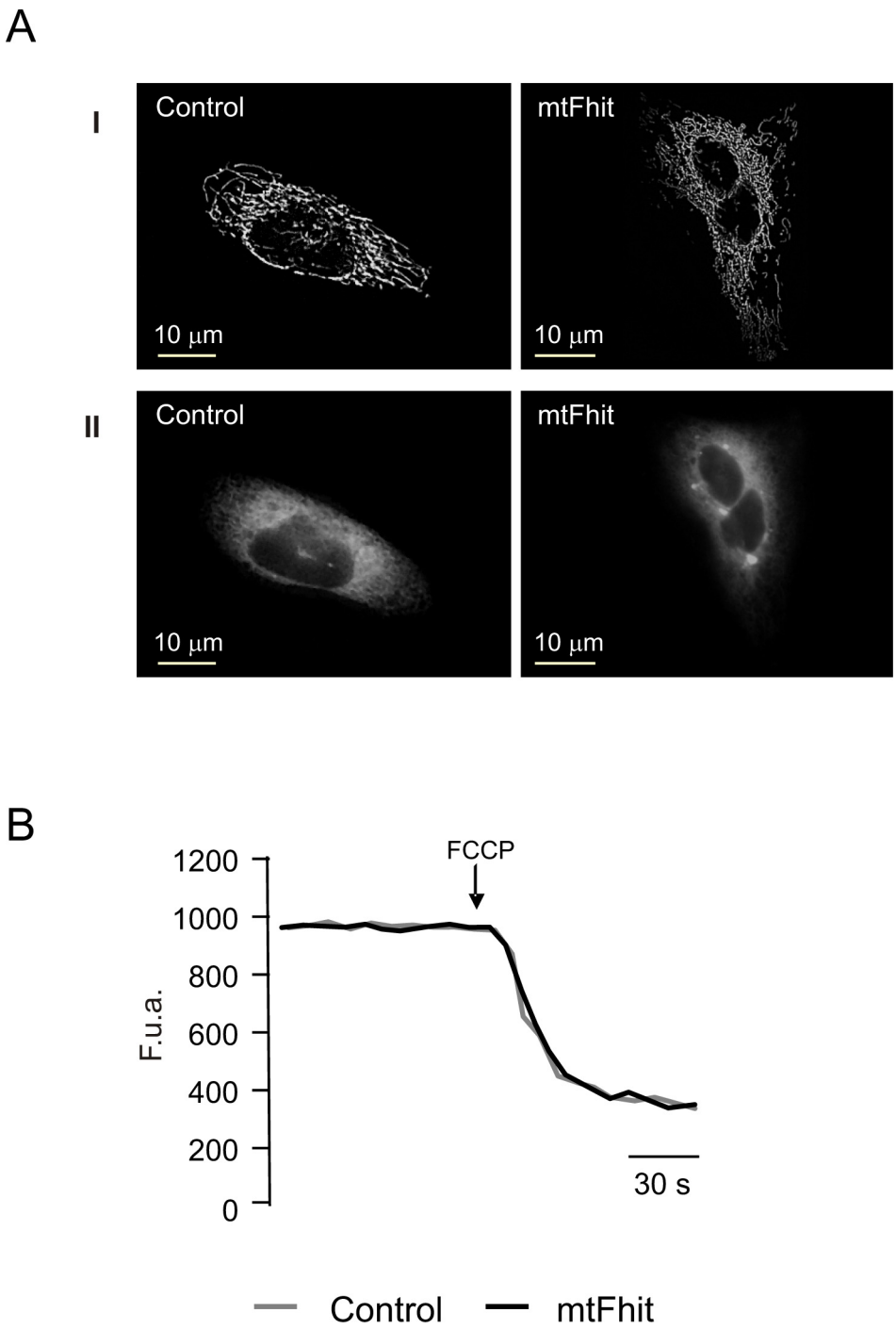

Fig. S3. (*A*) Morphological analysis of mitochondria (*I*) and ER (*II*) of control and mtFhit-expressing HeLa cells. (*B*) Kinetics of TMRM fluorescence of control and mtFhit-expressing cells. Where indicated (arrow), the $\Delta\Psi$ was collapsed by adding 1 μM FCCP.

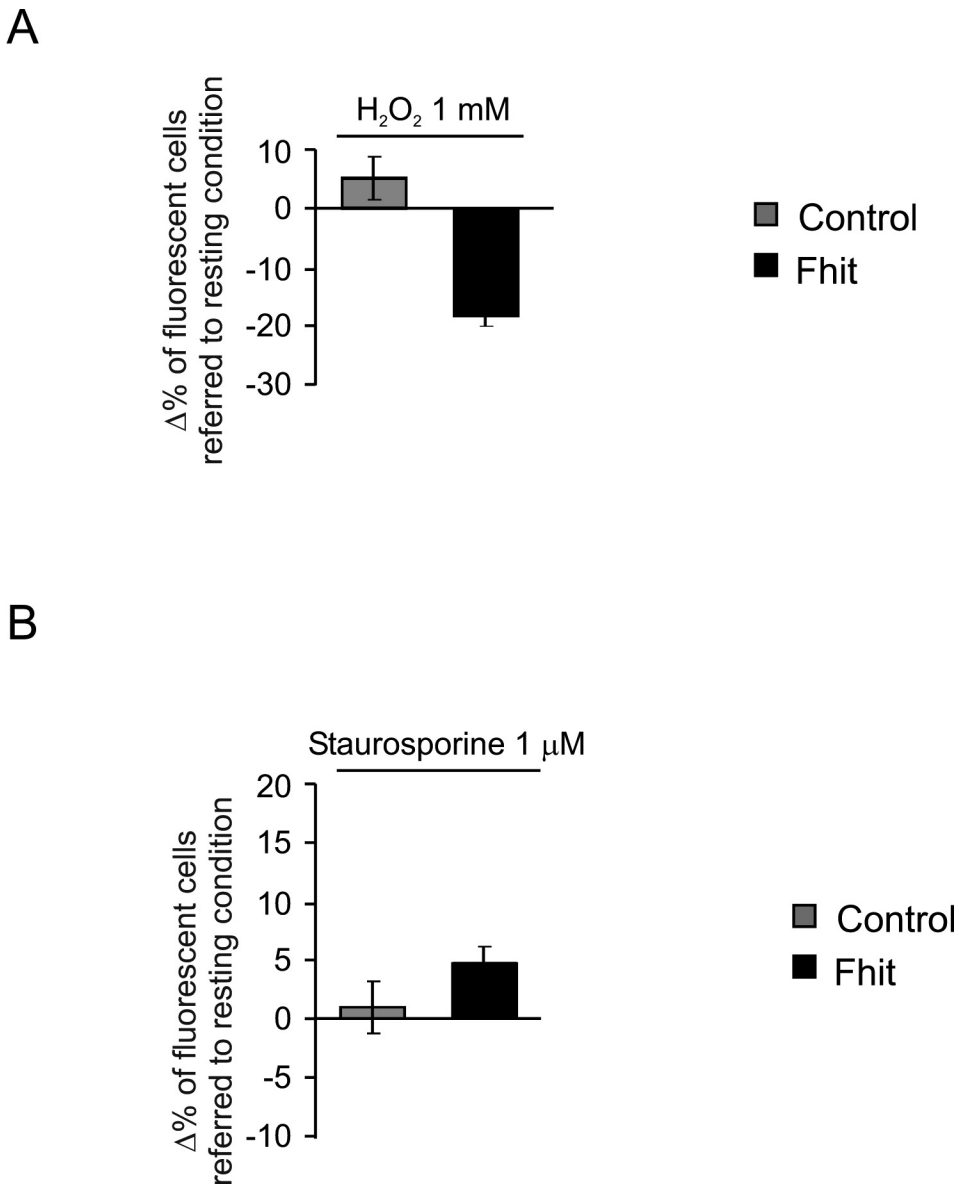

Fig. S4. Apoptotic counts carried out after treatment with 1 mM H_2O_2 (*A*) (control Δ% 5.78 ± 3.46 vs. Fhit −16.80 ± 1.58) and 1 μM staurosporin (*B*) (control Δ% 0.84 ± 3.10 vs. Fhit 4.39 ± 2.76).